03

NMR of monoclinic silver sulfide α-Ag_2S

© A.A. Valeeva[1], K.N. Mikhalev[2], E.V. Suvorkova[2], S.I. Sadovnikov[1], A.I. Gusev[1]

[1] Institute of Solid State Chemistry, Russian Academy of Sciences, Ural Branch, Yekaterinburg, Russia
[2] M.N. Mikheev Institute of Metal Physics, Ural Branch, Russian Academy of Sciences, Yekaterinburg, Russia

E-mail: valeevaar@mail.ioffe.ru, anibla_v@mail.ru

Received January 30, 2025
Revised January 31, 2025
Accepted February 2, 2025

^{109}Ag-NMR spectrometry was used to examine the structure of monoclinic α-Ag_2S powder. It was found that the ^{109}Ag-NMR spectrum of monoclinic α-Ag_2S had a form of a single narrow line, whose width slightly varied with temperature within 85−295 K. At a temperature below 200 K, a considerable growth of the isotropic component of shift tensor K_{iso} of ^{109}Ag nuclei is observed in the Ag_2S powder. Abnormally short time T_2 of ^{109}Ag spin-spin relaxation was detected. Simulation shows that, besides the acanthite described in the literature, other Ag_2S phases, that are derived from high-temperature argentite, β-Ag_2S, and have different structures, may be formed in silver sulfide as the temperature decreases. It is shown that the band structure of all predicted model Ag_2S phases has a band gap of 0.6−1.5 eV that is indicative of semiconductor properties of the phases.

Keywords: silver sulfide, ^{109}Ag isotope, isotropic shift, spin-spin relaxation time, predicted low-temperature Ag_2S phases.

DOI: 10.61011/PSS.2025.02.60673.21-25

1. Introduction

Nanostructured semiconductor sulfides are very important for various applications. Among them, large focus is made on nanostructured Ag_2S [1–3] that is a semiconductor at a temperature below 450 K and a superionic conductor at a temperature above 452 K.

According to the phase diagram of the Ag-S system [4,5], Ag_2S has three main polymorphous modifications. Low-temperature semiconductor α-Ag_2S phase with a monoclinic structure (acanthite) exists at a temperature below $\sim$ 450 K. Cubic β-Ag_2S phase (argentite) in equilibrium conditions exists in the temperature range of 452−859 K, has an body-centered (BCC) sublattice of S atoms and superionic conductivity. High-temperature cubic γ-Ag_2S phase with face-centered cubic sublattice of S atoms is stable at a temperature from $\sim$ 860 K to the melting temperature.

Potential use of nanostructured silver sulfide is most promising in micro/nanoelectronics, where Ag_2S/Ag heteronanostructures are used in nonvolatile memory and resistive switches. Their action is based on the reduction of Ag^+ to metallic Ag atoms, transformation of acanthite, α-Ag_2S, to argentite, β-Ag_2S, and appearance of conducting channel consisting of Ag and β-Ag_2S [6,7]. Due to the features of a band structure, Ag_2S/Ag hybrid heteronanostructures displayed high efficiency in heterogeneous catalysis and photocatalysis [8,9].

Ag_2S is used as an optical and electronic component (photovoltaic cells, photoconductors, biosensors and biomarkers, IR detectors) [10] and as an superionic conductor [11–13]. All types of nanostructured silver sulfide have considerable antibacterial activity. Ag_2S is used in photoswitches and oxygen sensors.

Ag_2S quantum dots demonstrate high photoluminescence and outstanding photostability. Therefore, Ag_2S quantum dots smaller than 3−4 nm may be used as luminophores or biomarkers for infrared radiation.

2. Results and discussion

Silver sulfide powders were synthesized by chemical deposition from $AgNO_3$, Na_2S and $Na_3C_6H_5O_7$ solutions in water. Solubility product K_{sp} of silver sulfide is small and is $K_{sp} = 6.3 \cdot 10^{-50}$ at 298 K [3], therefore, silver sulfide deposition occurs almost immediately. Procedure for synthesis of Ag_2S powders with the desired mean size of nanoparticles was previously described in detail in [3,14].

Synthesized silver sulfide powders were examined using the Shimadzu XRD-7000 diffractometer in Cu$K_{\alpha 1}$- radiation in the angle interval $2\theta = 20-95^\circ$ in $\Delta(2\theta) = 0.02^\circ$ steps and with good statistics. Determination of lattice parameters and final clarification of the synthesized silver sulfide powder structure were performed in X'Pert HighScore Plus software package [15]. Mean size D of particles (more precisely — coherent scattering regions (CSR)) in the synthesized microcrystalline silver sulfide powders was evaluated by X-ray diffraction according to diffraction reflection broadening $\beta(2\theta)$ using the dependence of reduced $\beta^*(2\theta) = [\beta(2\theta)\cos\theta]/\lambda$ on the scattering vector $s = (2\sin\theta)/\lambda$.

X-ray pattern of the sythesized monoclinic α-Ag_2S powder is shown in Figure 1. Many diffraction reflections of

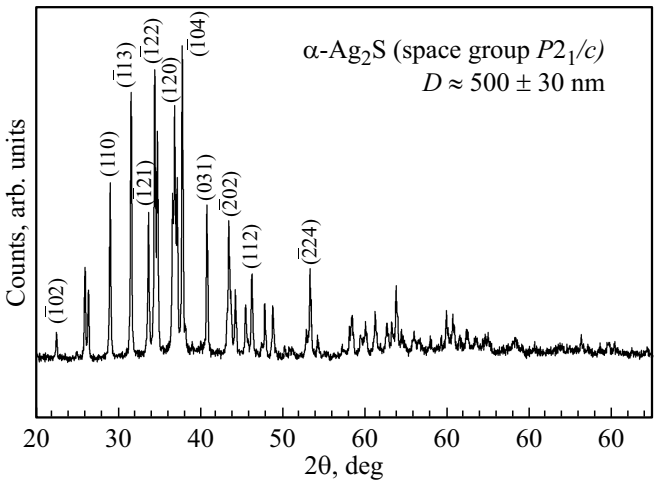

Figure 1. X-ray pattern of the microcrystalline monoclinic (space group $P2_1/c$) (a) α-Ag_2S powder at 295 K with particle size D equal to $\sim 500-30$ nm.

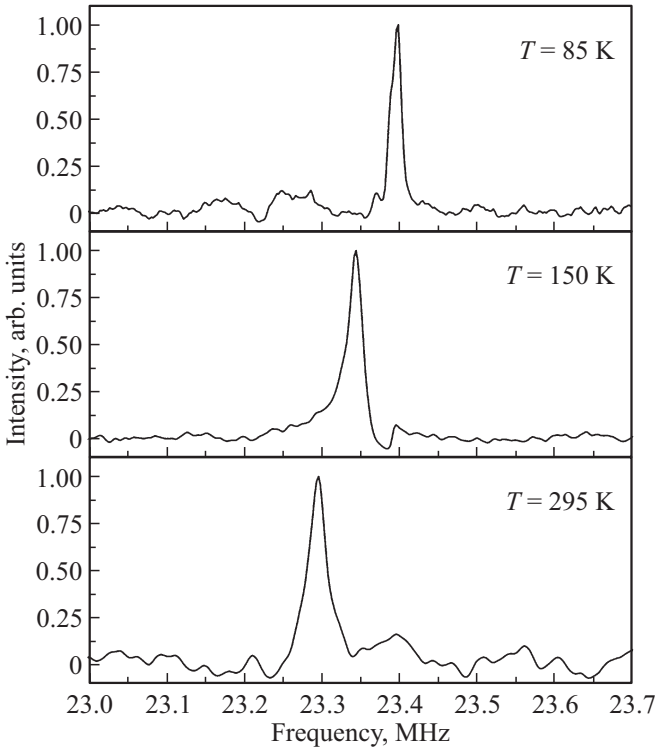

Figure 2. Typical ^{109}Ag-NMR spectra in the microcrystalline Ag_2S powder recorded at various temperatures in the range of 85–295 K.

the powder are overlapped. Quantitative clarification of the silver sulfide powder X-ray pattern and comparison with data of [14] showed that the observed set of diffraction reflections corresponded to monoclinic (space group $P2_1/c$) acanthite, α-Ag_2S. Evaluation of the CSR powder mean size conducted using nonoverlapping diffraction reflections showed that the size was approx. 500 nm, i. e. this was a microcrystalline powder.

^{109}Ag-NMR spectra in the microcrystalline Ag_2S powder were recorded on the AVANCE III 500 (Bruker) NMR spectrometer using a special low-temperature cell in a continuous-flow cryostat in the temperature range from 85 K to 295 K in the $H_0 = 11.7467$ T external magnetic field. NMR spectra were recorded using a standard double-pulse spin-echo sequence $\tau - t_{del} - \tau - t_{del}$-echo. Duration of the first pulse was set to $\tau = 2\,\mu$s. RF transmitter power was 400 W. NMR signal was recorded with delay between pulses $t_{del} = 20\,\mu$s. Spin-spin relaxation time was measured according to a standard procedure using the same sequence. In all cases, nuclear magnetization recovery was adequately described by a single exponential function [16].

To date, there is no literature data concerning ^{109}Ag-NMR spectral measurements of silver sulfide. ^{1}H- and ^{13}C-NMR spectral measurements of platelet silver thiolates (Ag-MPA) are shown in [17]. Thiolate complexes are used as capping agents in the synthesis of monodispersed silver, gold and other metal clusters.

Figure 2 shows typical ^{109}Ag-NMR spectra in microcrystalline Ag_2S powder recorded at a temperature from 85 K to 295 K in the 117.467 kOe external magnetic field. There are two naturally-occurring silver isotopes: ^{107}Ag (natural content 51.8 %) and ^{109}Ag (natural content 48.2 %), both isotopes have the nuclear spin $I = 1/2$. ^{109}Ag nuclei were chosen for measurements because their higher gyromagnetic ratio provides a better signal-to-noise ratio. ^{109}Ag-NMR spectrum of a microcrystalline sample (Figure 2) is a single narrow line with FWHM $\sim$ 20 kHz.

For the monoclinic crystalline structure of Ag_2S with equivalent positions of Ag atoms, particularly a single line shall be expected because nuclei with spin 1/2 has no quadrupole moment. Therefore only a central transition may be observed, i. e. the central part of spectrum associated with transition ($m = 1/2 \leftrightarrow -1/2$), where m is the magnetic quantum number [18,19]. Line width slightly varies with temperature in the range of 85–295 K. Analysis of ^{109}Ag-NMR spectra in the microcrystalline Ag_2S powder determined the shift tensor components. It was found that the shift was isotropic (within the measurement accuracy): $K_{iso} = 0.12(2)\,\%$ ($K_x = K_y = K_z$).

Temperature dependence of the isotropic component of shift tensor K_{iso} of ^{109}Ag nuclei in the microcrystalline Ag_2S powder is shown in Figure 3. Figure 3 shows that the shift of the NMR line (K_{iso}) varies slightly as the temperature decreases from 295 K to 200 K, whereas a significant shift growth is observed at a temperature below 200 K. Such behavior is not quite usual for a semiconductor compound without magnetic ions. The reason for the observed effect may be in any structural phase transition at $\sim$ 200 K in silver sulfide.

Temperature dependence of ^{109}Ag spin-spin relaxation time in Ag_2S is shown in Figure 4. Abnormally low T_2 is observed at 250 K (7 mks); it is even less at room temperature. Such times may be associated with fast dynamic processes near the Ag_2S ions. In particular, this

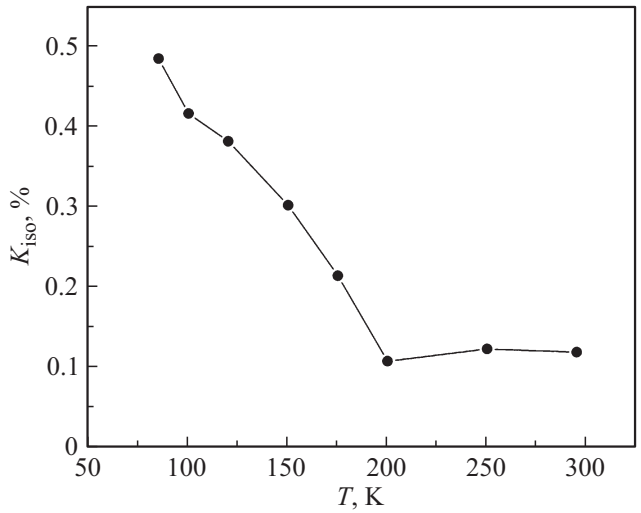

Figure 3. Temperature dependence of the isotropic component of shift tensor K_{iso} of ^{109}Ag nuclei in the microcrystalline Ag_2S powder.

may be associated with ionic mobility of silver that is typical of BCC argentite, β-Ag_2S.

Generally, the review of the ^{109}Ag-NMR spectra of the microcrystalline Ag_2S powder detected an abnormally low spin-spin relaxation time T_2 and significant temperature dependence of shift K_{iso}, which is not typical of the monoclinic semiconductor acanthite, α-Ag_2S. NMR is used for experimental examination of short-range order features, therefore the considerable growth of NMR line shift (K_{iso}) observed at a temperature below 200 K may result from a change of symmetry of the studied silver sulfide. In particular, the identified large growth of $K_{iso}$of the NMR line at a temperature below 200 K (Figure 3) indirectly suggests that there is a low-temperature Ag_2S phase at $T < 200$ K. Potential existence of low-temperature silver sulfide phases with cubic, tetragonal, orthorhombic, trigonal, monoclinic and triclinic symmetry was addressed previously in [20]. Possible model Ag_2S phases in [20] were sought using USPEX (Universal Structure Predictor: Evolutionary Xtallography) [21] described in detail in [22].

According to [2,23], the α-Ag_2S structure results from the distortion of the BCC sublattice of S atoms in the β-Ag_2S structure. Argentite — acanthite transformation is followed by the distortion of BCC sublattice of S atoms to a monoclinic sublattice and the shift of S and Ag atoms [3]. Transformation of the BCC argentite into the low-temperature monoclinic acanthite may be generally treated as ordering in the BCC sublattice of S atoms [24,25]. An argentite ordering option with formation of the monoclinic (space group $P2_1$) Ag_2S phase was proposed in [26]. In [20], it is shown that, besides the acanthite, other Ag_2S phases, that are derived from high-temperature argentite, β-Ag_2S, and have different structures, may be formed in silver sulfide as the temperature decreases.

Calculation of the enthalpy of formation of all given model Ag_2S phases [20] showed that the monoclinic α-Ag_2S structure (Figure 5, a) described in the literature [4,23,27] was not the only possible and the most energy-favorable low-temperature silver sulfide phase; its enthalpy of formation ΔH_f is equal to -0.033 eV per formula unit. The calculations gave the monoclinic (space group $P2_1/c$)

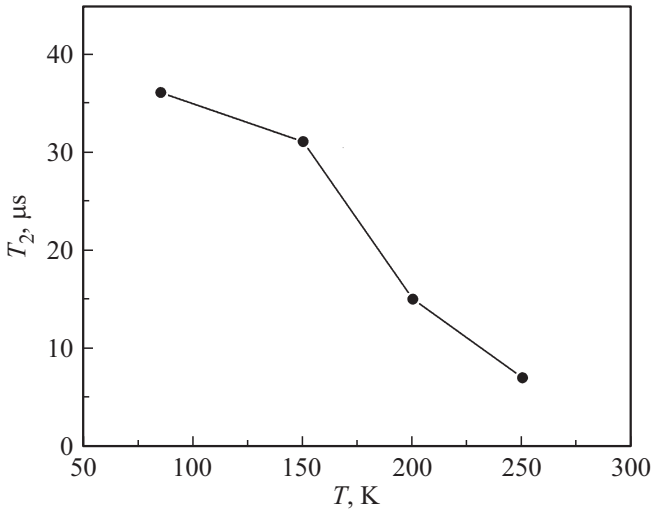

Figure 4. Temperature dependence of ^{109}Ag spin-spin relaxation time T_2 in microcrystalline Ag_2S powder.

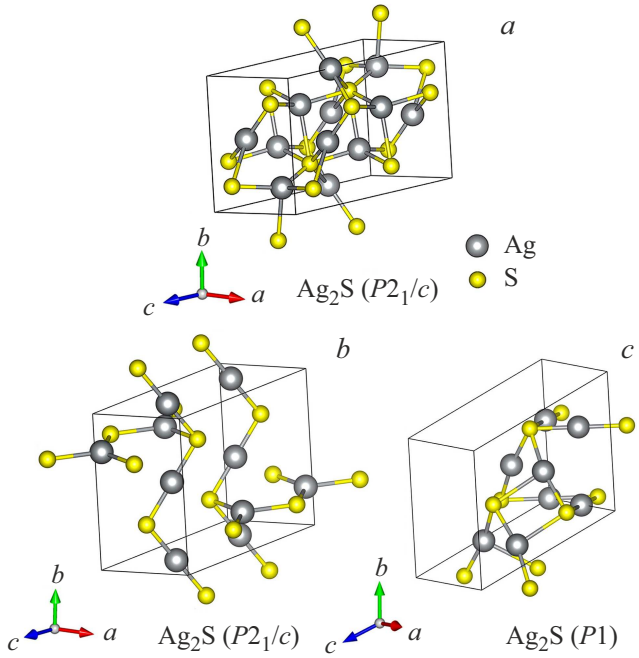

Figure 5. Lattice cell (a) of monoclinic (space group $P2_1/c$) α-Ag_2S according to [23,24] compared with the predicted model lattice cells: b — monoclinic (space group $P2_1/c$) Ag_2S phase with the enthalpy of formation $\Delta H_f = -0.219$ eV/formula units, which is the lowest among the predicted monoclinic structures, and c — triclinic (space group $P1$) Ag_2S phase with the lowest enthalpy of formation $\Delta H_f = -0.223$ eV/formula units.

Ag_2S phase (Figure 5, *b*) with a lower enthalpy of formation $\Delta H_f = -0.219$ eV per formula unit compared with the acanthite described in the literature and the triclinic (space group $P1$) Ag_2S phase (Figure 5, *c*) with the lowest enthalpy of formation $\Delta H_f = -0.223$ eV per formula unit in the ground state at $T = 0$ K and $P = 0$ Pa. Figure 5 shows the difference in the immediate S atom environment of Ag atoms in the monoclinic acanthite (Figure 5, *a*) and two model silver sulfide phases (Figure 5, *b* and *c*). Actually, according to the calculation [20], the interatomic distances Ag-S in these two model phases are slightly different from the interatomic distances Ag-S in monoclinic α-Ag_2S [3,23], which confirms some short-range order difference in them from the monoclinic acanthite and agrees with the obtained NMR measurements.

The band structure of all predicted model Ag_2S phases has a band gap from ~ 0.6 eV to ~ 1.5 eV that is indicative of semiconductor properties of the phases. Band gap E_g of triclinic (space group $P1$) Ag_2S is equal to 1.16 eV. Thus, theoretical calculations [20] of low-temperature silver sulfide phases confirm possible existence of the low-temperature Ag_2S phase at $T < 200$ K.

3. Conclusion

The ^{109}Ag-NMR method was first used to study the monoclinic α-Ag_2S powder. Measurements showed that the ^{109}Ag-NMR spectrum of monoclinic α-Ag_2S had a form of a single narrow line, whose width slightly varied at a temperature from 85 K to 295 K. Isotropic shift K_{iso} of the NMR line slightly varies as the temperature decreases from 295 K to 200 K, but at a temperature below 200 K a significant growth of the isotropic component of shift tensor K_{iso} of ^{109}Ag nuclei is observed in the Ag_2S powder. It is suggested that the observed effect may be associated with the structural phase transitions in silver sulfide at ~ 200 K.

Possible existence of low-temperature silver sulfide phases derived from high-temperature β-Ag_2S was addressed. The model calculations gave the monoclinic (space group $P2_1/c$) Ag_2S phase with a lower enthalpy of formation $\Delta H_f = -0.219$ eV per formula unit compared with the acanthite described in the literature and the triclinic (space group $P1$) Ag_2S phase with the lowest enthalpy of formation $\Delta H_f = -0.223$ eV per formula unit in the ground state at $T = 0$ K and $P = 0$ Pa. A band gap present in the band structure of all predicted model Ag_2S phases is indicative of their semiconductor properties.

Funding

The study was funded by the Russian Scientific Foundation (project № 19-73-20012-P, https://rscf.ru/en/project/19-73-20012/) at the Institute of Solid State Chemistry, Russian Academy of Sciences, Ural Branch using the equipment provided by the Physical and Technology Complex of the Institute of Metal Physics, Ural Branch, Russian Academy of Sciences.

Conflict of interest

The authors declare that they have no conflict of interest.

References

[1] A. Tang, Yu Wang, H. Ye, C. Zhou, C. Yang, X. Li, H. Peng, F. Zhang, Y. Hou, F. Teng. Nanotechnology **24**, *35*, 355602 (10) (2013). http://dx.doi.org/10.1088/0957-4484/24/35/355602
[2] S.I. Sadovnikov, A.I. Gusev. J. Mater. Chem. A **5**, *34*, 17676–17704 (2017). DOI: 10.1039/C7TA04949H
[3] S.I. Sadovnikov, A.A. Rempel, A.I. Gusev. Springer Intern. Publ. AG, Cham–Heidelberg (2018). 317 p.
[4] R.C. Sharma, Y.A. Chang. The Ag-S (silver-sulfur) system. Bull. Alloy Phase Diagr. *7*, *3*, 263–269 (1986).
[5] R.C. Sharma, Y.A. Chang. Ag-S (Silver-Sulphur). In: *Binary Alloy Phase Diagrams*. Ed. T.B. Massalski, H. Okamoto, L. Kacprzak. Metals Park (Ohio, USA): ASM Intern. Publ. (1990). P. 86–87.
[6] C.H. Liang, K. Terabe, T. Hasegawa, M. Aono. Nanotechnology **18**, *48*, 485202 (5) (2007). DOI: 10.1088/0957-4484/18/48/485202
[7] Z. Xu, Y. Bando, W. Wang, X. Bai, D. Golberg. ACS Nano **4**, *5*, 2515–2522 (2010). DOI: 10.1021/nn100483a
[8] M. Basu, R. Nazir, C. Mahala, P. Fageria, S. Chaudhary, S. Gangopadhyay, S. Pande. Langmuir **33**, *13*, 3178–3186 (2017). DOI: 10.1021/acs.langmuir.7b00029
[9] W. Yang, L. Zhang, Y. Hu, Y. Zhong, H.B. Wu, X.W. Lou. Angew. Chem. Int. Ed. **51**, *46*, 11501–11504 (2012). DOI: 10.1002/anie.201206715
[10] S. Kitova, J. Eneva, A. Panov, H. Haefke. J. Imaging Sci. Technol. **38**, *5*, 484–488 (1994).
[11] T. Minami. J. Non-Cryst. Solids **95–96**, *1*, 107–118 (1987). https://doi.org/10.1016/S0022-3093(87)80103-5
[12] S. Hull, D.A. Keen, D.S. Sivia, P.A. Madden, M. Wilson. J. Phys. Condens. Matter **14**, *41*, L9–L17 (2002). DOI: 10.1088/0953-8984/14/1/102
[13] W.P. Lim, Z. Zhang, H.Y. Low, W.S. Chin. Angew. Chem. Int. Ed. **43**, *42*, 5685–5689 (2004). https;//doi.org/10.1002/anie.200460566
[14] S.I. Sadovnikov, A.I. Gusev, A.A. Rempel. Superlatt. Microstr. **83**, 35–47 (2015). http://dx.doi.org/10.1016/j.spmi.2015.03.024
[15] X'Pert HighScore Plus.Version 2.2e (2.2.5). © 2009 PANalytical B.V. Almedo, the Netherlands.
[16] T.C. Farrar, E.D. Becker. Pulse and Fourier Transform NMR: Introduction to Theory and Methods. Academic Press, N.Y.–London (1971). 115 p.
[17] J. Wang, R. Graf, A. Riedinger. J. Materi. Chem. C **9**, *34*, 11079–11084 (2021). DOI: 10.1039/D1TC01983J
[18] A. Abraham. Yaderny magnetizm. Pod redaktsiei G.V. Skrotskogo. Inostr. Lit., M. (1963). 551 s. (in Russian).
[19] Ch.Slikter. Osnovy teorii magnitnogo rezonansa. Mir, M. (1981) (in Russian). 448 s. (in Russian).
[20] S.I. Sadovnikov, M.G. Kostenko, A.I. Gusev, A.V. Lukoyanov. ZhETF **165**, *3* 374–388 (2024). (in Russian). DOI: 10.31857/S0044451024030076
[21] Universal Structure Predictor: Evolutionary Xtallography. Manual. Version 9.4.4 (http://uspex-team.org)

[22] A.R. Oganov, C.W. Glass. J. Chem. Phys. **124**, *24*, 244704 (2006). https://doi.org/10.1063/1.2210932
[23] R. Sadanaga, S. Sueno. Mineralog. J. Japan. **5**, *2*, 124–148 (1967).
[24] S.I. Sadovnikov, A.I. Gusev. JETP Lett. **109**, *9*, 584–588 (2019). DOI: 10.1134/S0021364019090145
[25] O. Alekperov, Z. Jahangirli, R. Paucar. Phys. Stat. Sol. B **253**, *10*, 2049–2055 (2016). DOI: 10.1002/pssb.201552784
[26] S. Kashida, N. Watanabe, T. Hasegawa, H. Iida, M. Mori, S. Savrasov. Sol. State Ionics **158**, *1*, 167–175 (2003). https://doi.org/10.1016/S0167-2738(02)00768-3
[27] S.I. Sadovnikov, A.I. Gusev, A.A. Rempel. Superlat. Microstr. **83**, 35–47 (2015). http://dx.doi.org/10.1016/j.spmi.2015.03.024

Translated by E.Ilinskaya